Supplementary information

Achieving ultrahigh energy-storage capacity in $PbZrO_3$-based antiferroelectric capacitors based on optimization of property parameters

Xiaohui Liu,[a] Tongqing Yang*[a] and Weiping Gong[b]

[a] Key Laboratory of Advanced Civil Engineering Materials of the Ministry of Education, Functional Materials Research Laboratory, School of Materials Science and Engineering, Tongji University, 4800 Cao'an Road, Shanghai, 201804, China

[b] Guangdong Provincial Key Laboratory of Electronic Functional Materials and Devices, Huizhou University, Huizhou, 516001, Guangdong, China

E-mail: Yangtongqing@tongji.edu.cn

**Corresponding Author.*

Experimental procedure

The high-quality slurry, the second ball-milled PLSZT matrix powders, solvent (toluene/ethanol) and dispersant (phosphate ester) were ball-milled at 200 rpm for 12 h. Then, binder (polyvinyl butyral), plasticizer (polyethylene glycol-400/benzyl butyl phthalate) and homogenizer(cyclohexanone) were added and ball-milled for 12 h. And then, the bubbles were removed from the slurry in a defoaming machine. The prepared slurry with good liquidity was cast on a film-belt substrate by using a tape casting machine. The wet films were kept for 12 h at room temperature for desiccation. The ceramic thick films were cut to square with the diameter of 12 mm and the same thick films were pressed into square green bodies at 30 MPa and 70 ^{o}C by using a hot press mold. Finally, the samples were sintered to form ceramics. The thickness and electrode area of testing sample are 100 μm and 0.0314 cm^2, respectively.

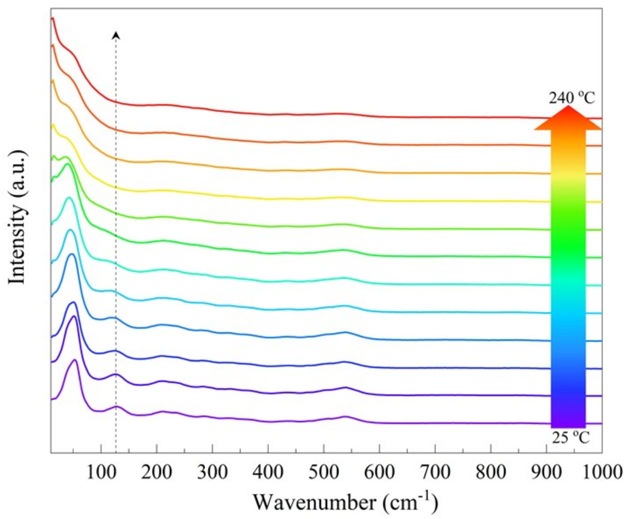

Fig. S1 Evolution of Raman spectra under different the temperature for PLSZT5 ceramic

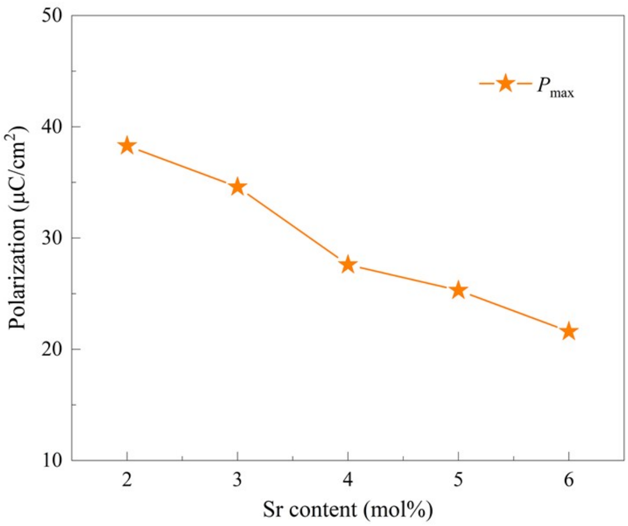

Fig. S2 The P_{amx} of for PLSZT ceramic with different Sr^{2+} contents under 40 kV/mm .

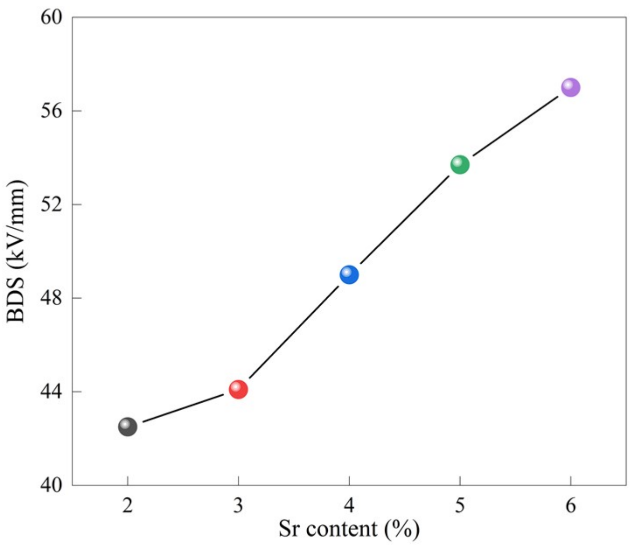

Fig. S3 The BDS of for PLSZT5 ceramic with different Sr^{2+} contents

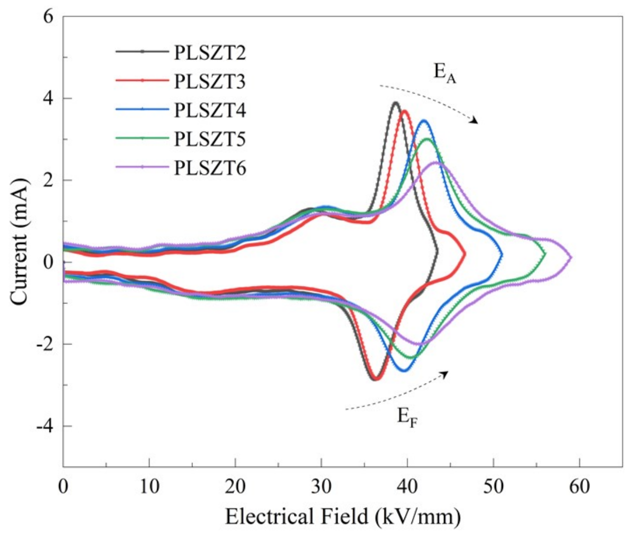

Fig. S4 The polarization current-electric field (I–E) loops of the PLSZT ceramic with different Sr^{2+} contents.

Table S1. The average ionic radii of A-site and B-site cation and tolerance factor in PLSZT ceramics

Composition	R_A-site	R_B-site	Tolerance factor
PLSZT2	0.1440	0.0719	0.954
PLSZT3	0.1437	0.0719	0.953
PLSZT4	0.1434	0.0719	0.952
PLSZT5	0.1431	0.0719	0.951
PLSZT6	0.1428	0.0719	0.949

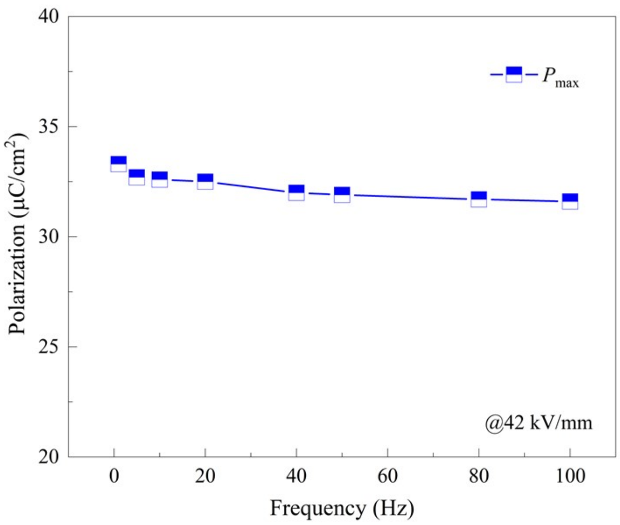

Fig. S5 The P_{amx} of for PLSZT5 ceramic from 1 to 100 Hz at 420 kV/cm

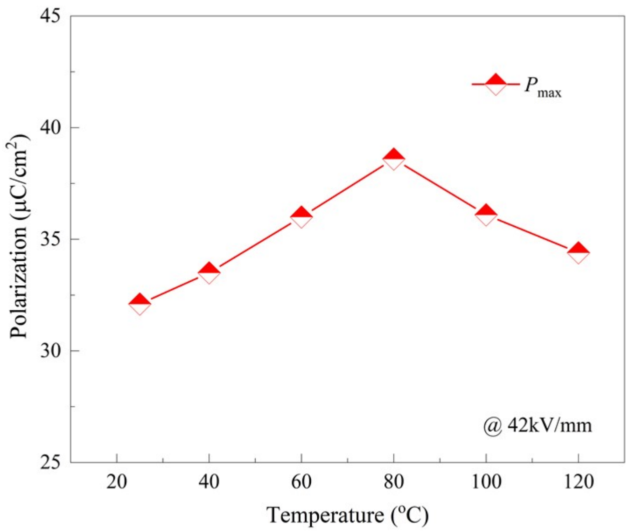

Fig. S6 The P_{amx} of for PLSZT5 ceramic from 25 to 120 ^{o}C at 420 kV/cm

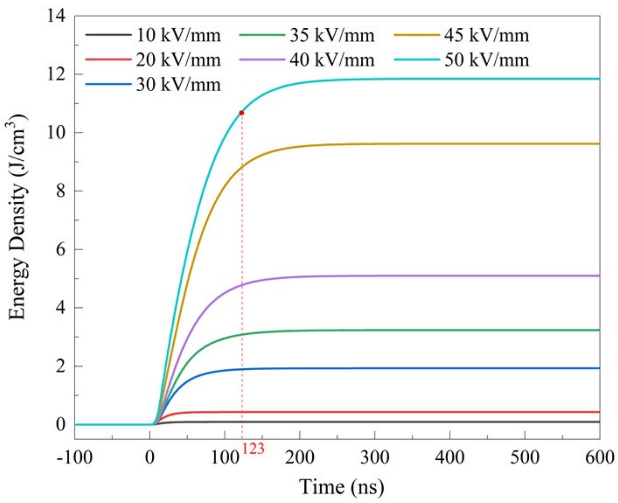

Fig. S7 The discharge current waveforms of the PLSZT5 ceramic with various electric fields.